

Synthesis of ZnO-nanoparticles by microwave assisted sol-gel method and its role in photocatalytic degradation of food dye Tartrazine (Acid Yellow 23)

Navid Assi¹; Parviz Aberoomand Azar^{1,*}; Mohammad Saber Tehrani¹; Syed Waqif Husain¹; Maher Darwish²; Sanaz pourmand³

¹Department of Chemistry, Science and Research Branch, Islamic Azad University, Tehran, Iran

²Department of Drug and Food Control, Faculty of Pharmacy, International Campus, Tehran University of Medical Sciences, Tehran, Iran

³Department of Chemistry, Amirkabir University of Technology (AUT), Tehran, Iran

Received 11 February 2017; revised 11 May 2017; accepted 09 June 2017; available online 14 June 2017

Abstract

ZnO- nanoparticles with an average particle size of 24 nm were successfully synthesized using the microwave assisted sol- gel technique. Structural and morphological properties of the nanoparticles were characterized by X-ray diffraction (XRD), Field emission scanning electron microscopy (FESEM), Energy disperse spectrum (EDS) and Fourier transform infrared spectroscopy (FTIR). The band gap energy was measured to be 3.27 eV. The photocatalytic degradation of tartrazine has been studied in aqueous solution under UV-C irradiation at different pH values, catalyst doses, and tartrazine concentration. Degradation of samples was monitored by a spectrophotometer. Results have shown that 95% of 50 mg L⁻¹ tartrazine was degraded in 120 min due to the photocatalytic degradation in presence of 0.02 g of ZnO-nanoparticles. The photocatalytic degradation kinetics has also been investigated. The experimental data were fitted very well in the pseudo-first-order kinetic and Langmuir-Hinshelwood models.

Keywords: Degradation; Kinetics; Photocatalytic; Tartrazine; ZnO-nanoparticles; X-ray diffraction (XRD).

How to cite this article

Assi N, Aberoomand Azar P, Saber Tehrani M, Husain SW, Darwish M, Pourmand S. Synthesis of ZnO-nanoparticles by microwave assisted sol-gel method and its role in photocatalytic degradation of food dye Tartrazine (Acid Yellow 23). *Int. J. Nano Dimens.*, 2017; 8 (3): 241-249.

INTRODUCTION

Wastewater from textile, paper, and some other industries contains residual dyes, which are not readily biodegradable. Tartrazine (C.I. Acid Yellow 23) as a typical representative of the group, is used as a cosmetic, drug and food coloring agent. It is considered highly toxic to humans and is found at high amounts in industrial effluents [1, 2]. Many methods have been reported for the removal of this compound from the environment including adsorption [3], microbial [4] or photocatalytic degradation [5], microwave assisted catalytic oxidation [6], electro-Fenton methods [5], electrocoagulation [7], electrochemical treatment [8], and advanced oxidation using UV/ H₂O₂ [9, 10]. Among these

methods, Heterogeneous photocatalysis is an important destructive technology which can lead to the total mineralization of most organic pollutants [11]. Some metal oxide semiconductors such as titanium dioxide (TiO₂), zinc oxide (ZnO), Zirconium Oxide (ZrO₂), tungsten oxide (WO₃), strontium titanate (SrTiO₃) and hematite (α -Fe₂O₃) are purported to be dynamic photocatalysts. ZnO is a widely studied metal oxide for applications such as solar cells, sensors, ultraviolet nanolasers, and blue-light-emitting diodes (LEDs) [12]. It is a wide band gap ($E_g=3.3$ eV) metal oxide semiconductor with piezoelectric and optical properties in the UV range [13]. An increasing number of scientific reports have appeared on using ZnO in photocatalytic degradation of organic compounds

* Corresponding Author Email: parvizaberoomand@gmail.com

[14, 15]. ZnO-nanoparticles can be synthesized by a number of techniques including sol-gel processing [16-19], homogeneous precipitation [20], mechanical milling [21], organometallic synthesis [22], microwave [23], spray pyrolysis [24, 25], thermal evaporation [26], and mechanochemical synthesis [27].

We report here the studies on photocatalytic degradation of tartrazine in the presence of UV-C irradiation using ZnO-nanoparticles synthesized by a microwave assisted sol-gel technique. The synthesized ZnO-nanoparticles were characterized by XRD, FESEM, FTIR, EDS and the band gap energy was also calculated. Furthermore, the optimum conditions of photocatalytic reaction such as ZnO-nanoparticles loading, pH, and initial tartrazine concentration were inspected and realized. Finally, reaction kinetics of tartrazine degradation was investigated.

EXPERIMENTAL

Materials and methods

Tartrazine dye (acid yellow 23), with the structure shown in Fig. 1, was obtained from (Sigma-Aldrich, 85%). Zinc acetate dihydrate ($\text{Zn}(\text{CH}_3\text{COO})_2 \cdot 2\text{H}_2\text{O}$), Ethylene glycol ($\text{C}_2\text{H}_6\text{O}_2$), Hydrochloric acid (HCl) and Ammonia solution (25% v/v) were obtained from Merck (Germany). All materials were of analytical grade. Deionized water was used for the preparation of all samples. The degradation of tartrazine was monitored using UV-Vis spectrophotometer (Cary 100 UV-Vis spectrophotometer).

Preparation of ZnO-nanoparticles

The synthesis of ZnO-nanoparticles by the microwave assisted sol-gel technique was as

follow, a clear solution of 4 g of zinc acetate dihydrate ($\text{Zn}(\text{CH}_3\text{COO})_2 \cdot 2\text{H}_2\text{O}$) in 30 ml ethylene glycol was prepared with a Heidolph homogenizer at 7000 rpm for 5 min. The pH of the solution was adjusted to 6. Then, the solution was stirred with a magnetic stirrer (600 rpm) for 3 hours at 120°C . The obtained gel was exposed to a microwave irradiation at a power of 600 W for 10 min. The resultant powder was calcined at 450°C for 2 h to produce the ZnO-nanoparticles. The sheet chart explaining the procedure of the preparation of ZnO-nanoparticles is shown in Fig. 2.

Photocatalytic activity Procedures

To study the photocatalytic degradation, 100 ml solution containing 50 mg L^{-1} tartrazine was prepared and the pH was adjusted to 6. Next, 0.02 g of the ZnO-nanoparticles was added with the solution placed at a distance of 10 cm from the UV-C lamp (30 W) for 120 min with continuous agitation. At certain reaction intervals, 5 ml samples were taken out and then centrifuged at 1000 rpm for 2 min to remove any suspended solid. The remained concentration of tartrazine was determined with UV-Vis spectrophotometer. According to the Beer-Lambert law, the concentration of tartrazine is proportional to the absorbance of tartrazine, so the degradation efficiency of tartrazine was calculated by Eq. 1. [28]:

$$\text{Degradation} = \frac{C_0 - C}{C_0} \times 100 = \frac{A_0 - A}{A_0} \times 100 \quad (1)$$

Where A_0 , A, and C_0 , C are the absorbance and concentration of tartrazine when the reaction time is 0 and t, respectively [29, 30].

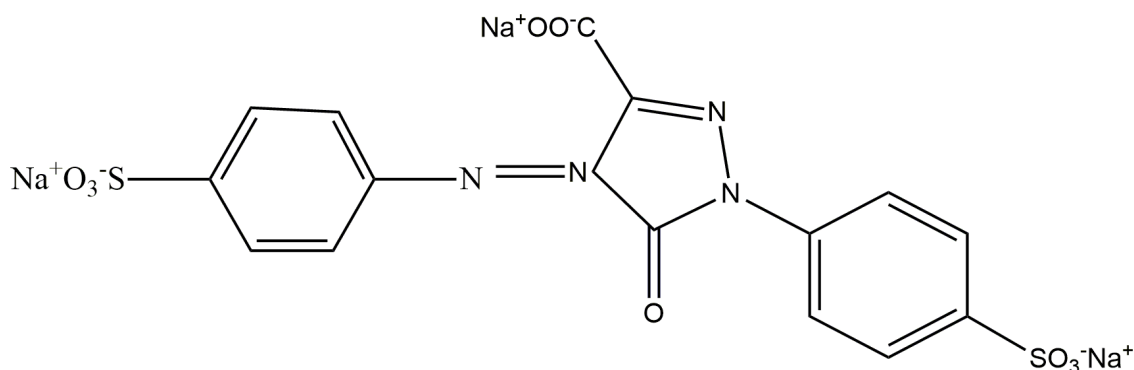


Fig. 1: Structure of Tartrazine dye (Acid yellow 23).

RESULTS AND DISCUSSION

Assessment of ZnO-nanoparticles

XRD analysis was conducted on a D8-Advance (Product Cooperation Bruker AXS and Siemens) fitted with a Cu-K α radiation tube. X-ray diffractogram (Fig. 3) exhibited peaks well matched with JCPDS card No. 03-065-3411. This revealed single phase ZnO-nanoparticles with hexagonal crystal system. The amount of average crystallite size was estimated to be 27 nm by Scherrer equation (Eq. 2)

$$D = 0.89 \lambda / \beta \cos \vartheta \quad (2)$$

Where D is crystallite size, λ is the wavelength of X-ray, β is the modified FWHM, and ϑ is the reflection angle. The crystallinity percentage was calculated 75% from net to total area ratio.

FTIR spectrum in the range 4000-400 cm^{-1} of ZnO-nanoparticles was recorded in transmission mode (Thermo Nicolet 8700 FTIR) on powder samples that were ground with KBr and compressed into a pellet. The spectrum is illustrated in Fig. 4. The sharp absorption peak at 455.23 cm^{-1} is assigned to the metal-O stretching vibration. The peak at 1628.53 cm^{-1} refers to COO-metal bond and the broad absorption at about 3436.91 cm^{-1} assigned to the OH group which agree well with the results reported in the literature [30, 31].

FESEM microscope image to illustrate the morphology of ZnO-nanoparticles is shown in Fig. 5-a. The image confirmed the sizes of the particles in nanometer range (24 nm) with high shape and size uniformity. The EDX spectrum of ZnO by sol-gel method is presented in Fig. 5-b. The result indicates that the powder contains zinc and oxygen without any impurities.

Photocatalytic efficiency of ZnO nanoparticles

As Fig. 6 displays, there was no significant degradation with ZnO in a dark place (32%) or with UV-C irradiation alone without the present of ZnO (10%). The concomitant presence of ZnO-nanoparticles and UV-C irradiation resulted in almost complete degradation of tartrazine (95%) within 120 min. These results imply that ZnO-nanoparticles presence strongly influenced the photodegradation of tartrazine under the UV-C light.

Effect of catalyst weight

With an increase of ZnO-nanoparticles weight from 0.02 to 0.04 g the percentage of degradation increased from 95 to 100 in 120 min irradiation

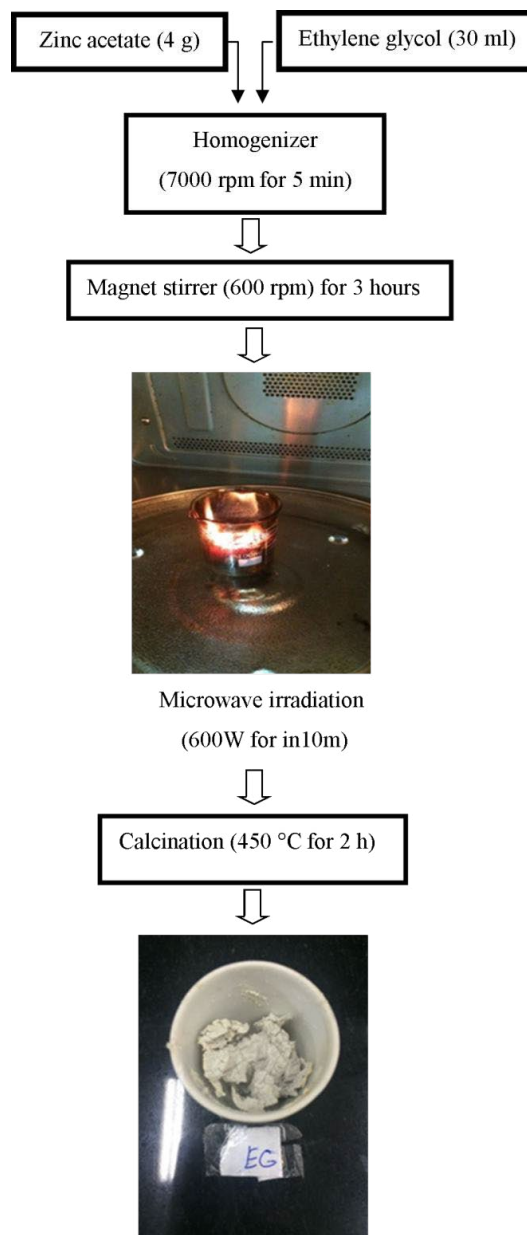


Fig. 2: Flow sheet of sol-gel method to prepare nanocrystalline ZnO.

time. After that the increase in ZnO-nanoparticles weight from 0.04 to 0.08 g did not affect the degradation significantly and, as shown in Fig. 7, at a higher amount of ZnO-nanoparticles (0.08 g), less photocatalytic degradation (63%) was observed. When the dose of ZnO catalyst increased above the limiting value (0.04 g), the total active surface area also increased, but there was a decrease in UV light penetration due to the increased suspension turbidity as result of the

excess catalyst particles in the solution [31-34]. Thus, to prevent this disadvantage property, 0.04 g of ZnO nanoparticles was used for all the following photocatalytic degradation studies.

Effect of initial dye concentration

Fig. 8 illustrates the effect of initial tartrazine concentration on photocatalytic degradation. The study was performed by varying the initial

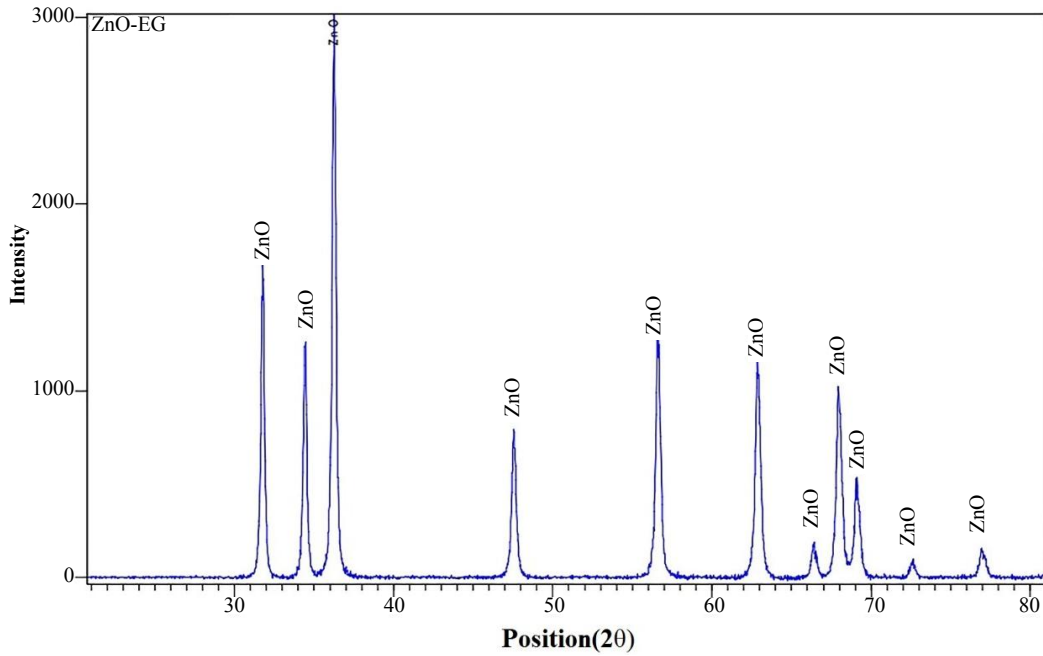


Fig. 3: X-ray diffraction pattern of ZnO- nanoparticles.

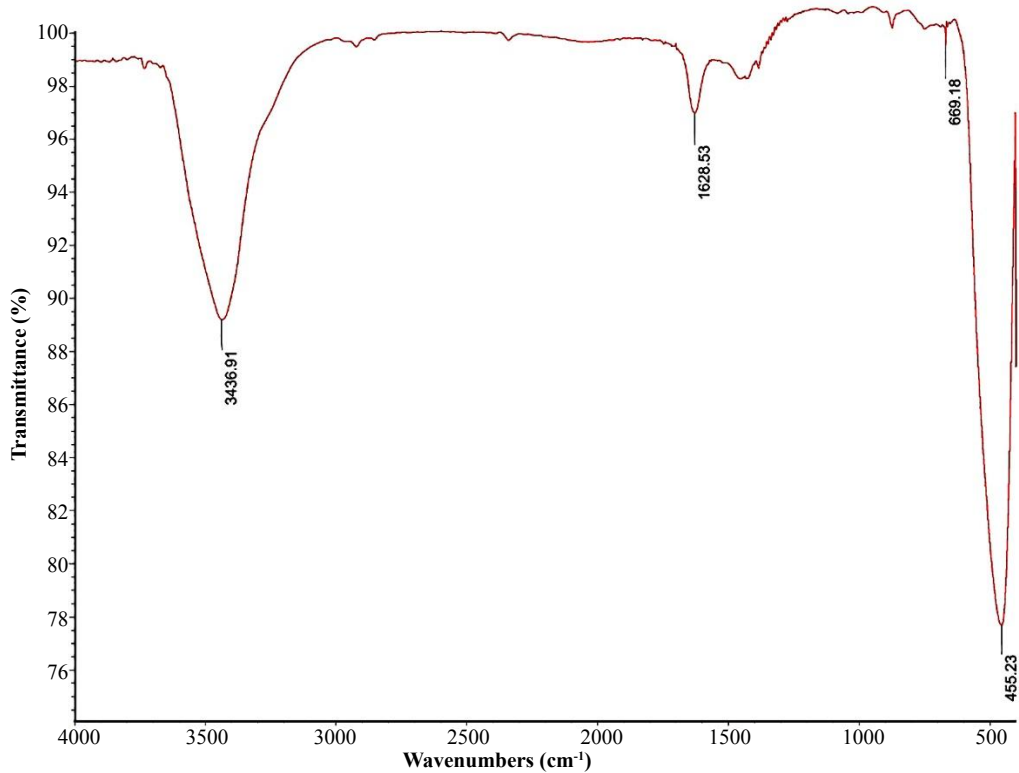


Fig. 4: FTIR transmission spectrum of ZnO- nanoparticles synthesized by microwave assisted sol- gel technique.

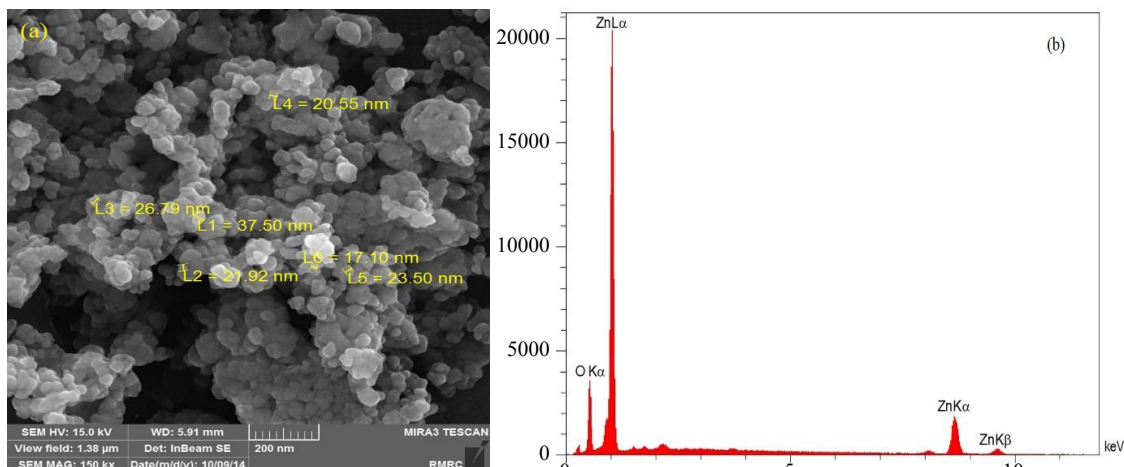


Fig. 5: a) The FESEM image and b) EDS of the ZnO- nanoparticles synthesized by microwave assisted sol- gel technique.

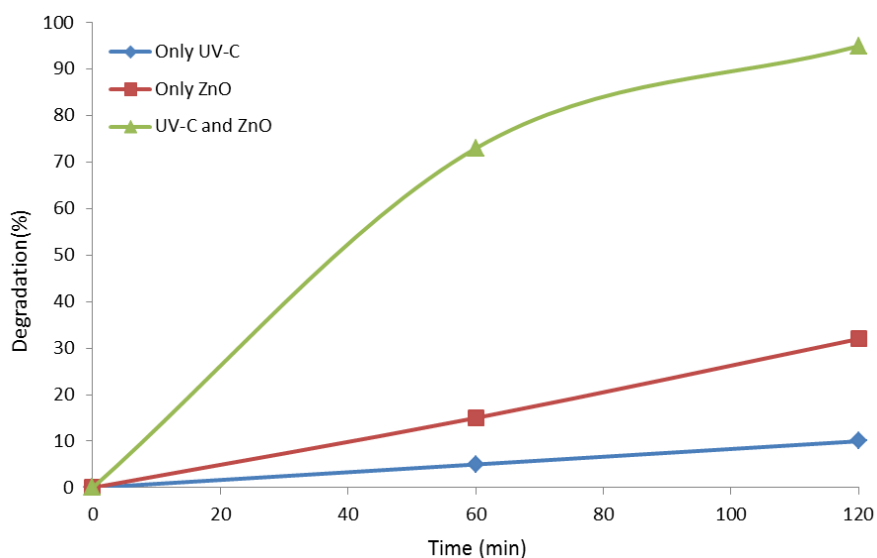


Fig. 6: Effect of UV-C light and 0.02 g of ZnO nanoparticles on the photocatalytic degradation of 50 mg L⁻¹ tartrazine at pH= 6.

concentration values, 20-200 mgL⁻¹ and measuring the absorbance decay in 120 min with 0.02 g ZnO- nanoparticles. The absorbance decay expressed as tartrazine concentration showed 95% of degradation at 50 mgL⁻¹. It is well-known that as initial concentration increases, more and more dye molecules are adsorbed on the surface of nanoparticles, the generation of hydroxyl radicals will be reduced since there are only fewer active sites for adsorption of hydroxyl ions and the generation of hydroxyl radicals. Hence, the absorption of photons by the catalyst decreases and, consequently, the photocatalytic degradation rate is reduced [2, 28, 35-37].

Effect of pH

The effect of pH on the photocatalytic degradation of a 50 mg L⁻¹ tartrazine solution in presence of 0.02 g ZnO-nanoparticles was explored. The degradation was monitored in a pH range 2.0 to 11.0 (the initial pH value was adjusted with HCl and Ammonia solution (25% v/v)) and is depicted in Fig. 9. In this study, pH= 6 was assessed to be the best pH for the tartrazine photocatalytic degradation. ZnO has a zero-point charge at about pH=9 and is positive charged in pH 5-7. Tartrazine has three O-Na sites, so this compound is negatively charged. Therefore, at pH=6, positive ZnO nanoparticles have high

degree of adsorption with negative tartrazine due to electrostatic attraction [38]. The decrease in the photocatalytic degradation of tartrazine at acidic pH may be due to the dissolution of ZnO-nanoparticles at low pH. In acidic medium, The ZnO nanoparticles were disappeared. At higher pHs, there was an excess of hydroxyl anions, which facilitate photogeneration of hydroxyl radicals [38-42].

Kinetics of photocatalytic degradation

The photocatalytic degradation of tartrazine in the range of 20-200 mgL⁻¹ containing 0.02 g ZnO-nanoparticles in the pH of 6, obeyed the pseudo-first-order kinetics as described by Eq. (3).

$$D = 0.89 \lambda / \beta \cos \theta \tag{3}$$

Where C₀ is the equilibrium concentration of tartrazine, C is the concentration at time t (min) and k is the pseudo-first-order rate constant.

Linear plots related to -ln(C/C₀) versus t (min) between tartrazine concentration and irradiation times for photodegradation are shown in Fig. 10. It can be observed that k value ranged between 0.0447 and 0.0035 for different tartrazine concentrations [36].

Sobana et al. [43] have used the Langmuir-Hinshelwood equation to analyses of the heterogeneous photocatalytic reaction successfully. The modified Langmuir-Hinshelwood equation is given in Eq.4:

$$-\ln \frac{C}{C_0} = kt \tag{4}$$

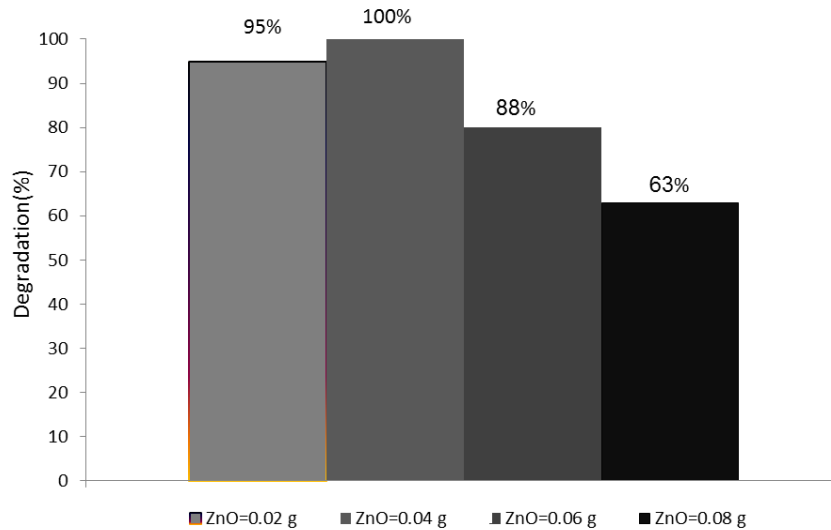


Fig. 7. Effect of ZnO- nanoparticles weight on photocatalytic degradation of 50 mgL⁻¹ tartrazine concentration in pH=6.

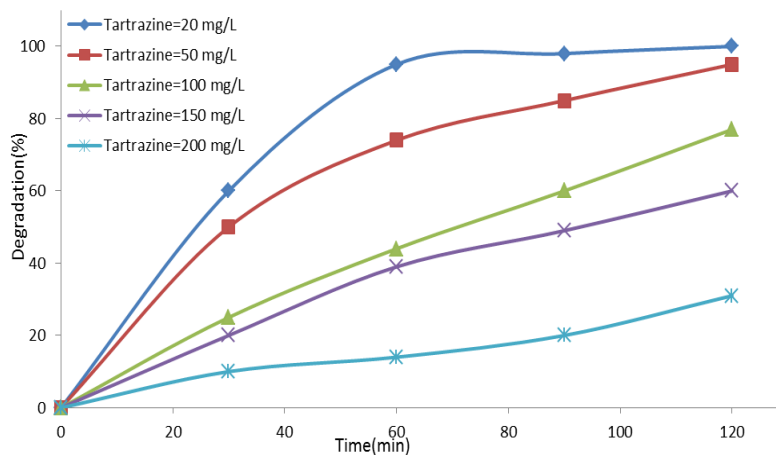


Fig. 8: The effect of initial tartrazine concentration in the present of 0.02 g ZnO in pH= 6.

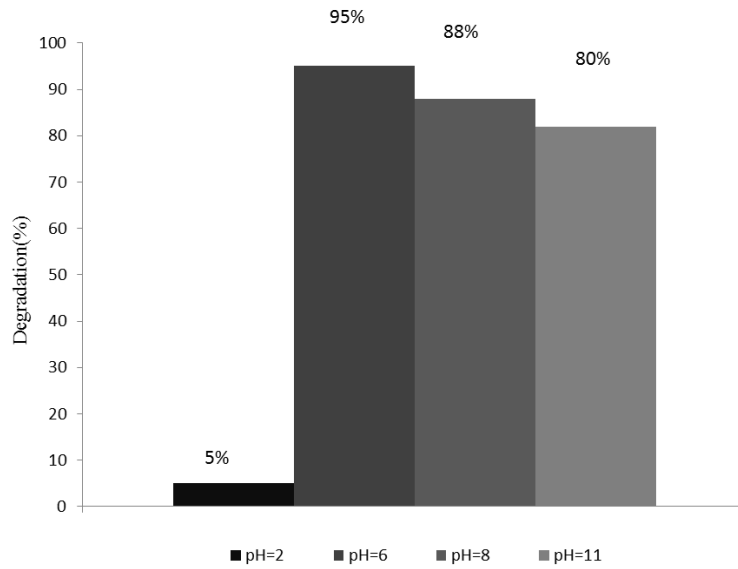


Fig. 9: Effect of initial pH on photocatalytic degradation of 50 mgL⁻¹ tartrazine in present of 0.02 g nano ZnO.

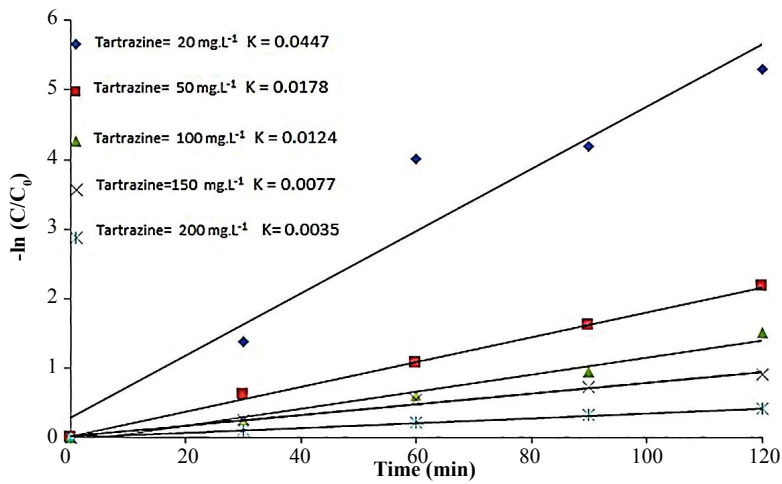


Fig. 10: linear Plots of $-\ln(C/C_0)$ versus time for tartrazine in the range of 20-200 mg/L, 0.02 g ZnO- nanoparticles in pH= 6.

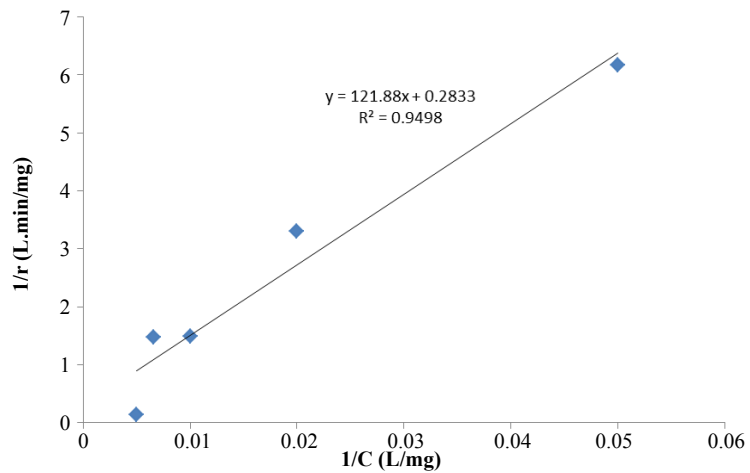


Fig. 11: A plot of $1/r$ against $1/C$ for the catalysis of tartrazine.

This equation can be rearranged as Eq.5:

$$r = \frac{K_L - K_{ads} [C]}{1 + K_{ads} [C]} \quad (5)$$

where r is the reaction rate ($\text{mgL}^{-1} \text{min}^{-1}$), k_{L-H} is the true rate constant ($\text{mg L}^{-1} \text{min}^{-1}$) including parameters such as catalyst loading, photon flux, and oxygen coverage, K_{ads} is the adsorption coefficient of tartrazine on the ZnO- nanoparticles ($\text{mg}^{-1} \text{L}$) and $[C]$ is the concentration of tartrazine (mgL^{-1}) at time t (min). The applicability of Langmuir-Hinshelwood equation for the photocatalytic degradation has been confirmed by the linear plot obtained by plotting the reciprocal of initial rate ($1/r$) against reciprocal of initial concentration ($1/C$) as shown in Fig. 11 with an R^2 value of 0.9498. The values of k_{L-H} and K_{ads} were $3.529 \text{ mg/L} \cdot \text{min}$ and $5.8 \times 10^{-4} \text{ L/mg}$, respectively, indicating that photocatalytic degradation was a dominant factor when compared to pollutant adsorption onto the surface of ZnO-nanoparticles [2, 37].

Band gap energy

The band gap energy (E_g) was evaluated from the UV-Vis spectrophotometer. ZnO-nanoparticles were dispersed in 10 mL ethanol and ultrasonicated for 10 min. The cutoff of the ZnO-nanoparticles was obtained from the absorption and reflection UV-Vis spectrum, and the E_g was calculated by the Eq.6:

$$\frac{1}{r} = \frac{1}{K_{L-H} K_{ads} [C]} + \frac{1}{K_{L-H}} \quad (6)$$

Where E_g is the direct band gap energy and λ is the cut off the ZnO- nanoparticles. The optical band gap of ZnO- nanoparticles estimated to be 3.27 eV in line with literature. [31, 34, 43-45].

CONCLUSIONS

ZnO-nanoparticles were synthesized successfully by microwave-assisted sol-gel technique using ethylene glycol. The average particle size, crystallinity, and band gap were calculated as 24 nm, 75% and 3.27 eV, respectively. Photocatalytic degradation of tartrazine was evaluated and the effect of the initial concentration, amount of photocatalyst loading and pH has been investigated. Kinetic of photocatalytic degradation was studied and data were fitted very well in the pseudo-first-order kinetic and Langmuir-Hinshelwood models.

CONFLICT OF INTEREST

The authors declare that there is no conflict of interests regarding the publication of this manuscript.

REFERENCES

- [1] Hess E. V., (2002), Environmental chemicals and autoimmune disease: Cause and effect. *Toxicolo.* 181: 65-70.
- [2] Behnajady M., Modirshahla N., Hamzavi R., (2006), Kinetic study on photocatalytic degradation of CI Acid Yellow 23 by ZnO photocatalyst. *J. Hazard. Mater.* 133: 226-232.
- [3] O'Connor O. A., Young, L., (1989), Toxicity and anaerobic biodegradability of substituted phenols under methanogenic conditions. *Environ. Toxicol. Chem.* 8: 853-862.
- [4] Dieckmann M. S., Gray K. A., (1996), A comparison of the degradation of 4-nitrophenol via direct and sensitized photocatalysis in TiO_2 slurries. *Water Res.* 30: 1169-1183.
- [5] O'turan M. A., Peiroten J., Chartrin P., Acher A. J., (2000), Complete destruction of p-nitrophenol in aqueous medium by electro-Fenton method. *Environ. Sci. Technol.* 34: 3474-3479.
- [6] Bo L., Zhang Y., Quan X., Zhao B., (2008), Microwave assisted catalytic oxidation of p-nitrophenol in aqueous solution using carbon-supported copper catalyst. *J. Hazard. Mater.* 153: 1201-1206.
- [7] Modirshahla N., Behnajady M., Mohammadi-Aghdam S., (2008), Investigation of the effect of different electrodes and their connections on the removal efficiency of 4-nitrophenol from aqueous solution by electrocoagulation. *J. Hazard. Mater.* 154: 778-786.
- [8] Canizares P., Saez C., Lobato J., Rodrigo, M., (2004), Electrochemical treatment of 4-nitrophenol-containing aqueous wastes using boron-doped diamond anodes. *Ind. Eng. Chem. Res.* 43: 1944-1951.
- [9] Chang Y.-C., Chen D.-H., (2009), Catalytic reduction of 4-nitrophenol by magnetically recoverable Au nanocatalyst. *J. Hazard. Mater.* 165: 664-669.
- [10] Chen C.-C., Fan H.-J., Jan J.-L., (2008), Degradation pathways and efficiencies of acid blue 1 by photocatalytic reaction with ZnO nanopowder. *J. Phys. Chem.* 112: 11962-11972.
- [11] Bhatkhande D. S., Kamble S. P., Sawant S. B., Pangarkar V. G., (2004), Photocatalytic and photochemical degradation of nitrobenzene using artificial ultraviolet light. *Chem. Eng. J.* 102: 283-290.
- [12] Sadeghi B., (2014), Preparation of ZnO/Ag nanocomposite and coating on polymers for anti-infection biomaterial application. *Spectrochim Acta A Mol Biomol Spectrosc.* 118: 787-792.
- [13] Ghane M., Sadeghi B., Jafari A., Paknejhad A., (2010), Synthesis and characterization of a Bi-Oxide nanoparticle ZnO/CuO by thermal decomposition of oxalate precursor method. *Int. J. Nano Dimens.* 1: 33-40.
- [14] Assi N., Sharif A. M., Naeini, Q. M., (2014), Synthesis, characterization and investigation photocatalytic degradation of Nitro Phenol with nano ZnO and ZrO_2 . *Int. J. Nano Dimens.* 5: 387-391.
- [15] Assi N., Sharif A. M., Bakhtiari H., Naeini Q. M., (2014),

- Photo catalytic property of ZnO and Mn-ZnO nanoparticles in removal of Cibacet Turquoise blue G from aquatic solution. *Int. J. Nano Dimens.* 5: 145-154.
- [16] Chu S.-Y., Yan T.-M., Chen S.-L., (2000), Characteristics of sol-gel synthesis of ZnO-based powders. *J. Mater. Sci. Lett.* 19: 349-352.
- [17] Assi N., Mohammadi A., Sadr Manuchehri Q., Walker R. B., (2014), Synthesis and characterization of ZnO nanoparticle synthesized by a microwave-assisted combustion method and catalytic activity for the removal of ortho-nitrophenol. *Desalination and Water Treatment.* 52: 1-10.
- [18] Gholipur R., Bahari A., Ebrahimzadeh M., (2017), Deposition of nanostructured $Zr_xLa_{1-x}O_2$ thin films on P-type Si (100) substrate by the sol-gel route. *Silicon.* 9: 173- 181.
- [19] Ebrahimzadeh M., Bahari A., (2016), Structural and Electrical Properties of $Zr_xY_{1-x}O_2$ nanocomposites for gate dielectric applications. *J. Electron. Mater.* 45: 235-244.
- [20] Damonte L., Zélis L. M., Soucase B. M., Fenollosa M. H., (2004), Nanoparticles of ZnO obtained by mechanical milling. *Powder Technol.* 148: 15-19.
- [21] Kahn M. L., Monge M., Collière V., Senocq F., Maisonnat A., Chaudret B., (2005), Size-and shape-control of crystalline Zinc Oxide nanoparticles: A new organometallic synthetic method. *Adv. Funct. Mater.* 15: 458-468.
- [22] Komarneni S., Bruno M., Mariani E., (2000), Synthesis of ZnO with and without microwaves. *Mater. Res. Bull.* 35: 1843-1847.
- [23] Hong R., Li J., Chen L., Liu D., Li H., Zheng Y., Ding J., (2009), Synthesis, surface modification and photocatalytic property of ZnO nanoparticles. *Powder Technol.* 189: 426-432.
- [24] Tani T., Mädler L., Pratsinis S. E., (2002), Homogeneous ZnO nanoparticles by flame spray pyrolysis. *J. Nanopart. Res.* 4: 337-343.
- [25] Dai Z. R., Pan Z. W., Wang Z. L., (2003), Novel nanostructures of functional oxides synthesized by thermal evaporation. *Adv. Funct. Mater.* 13: 9-24.
- [26] Ao W., Li J., Yang H., Zeng X., Ma X., (2006), Mechanochemical synthesis of zinc oxide nanocrystalline. *Powder Technol.* 168: 148-151.
- [27] Abdollahi Y., Abdollah A. H., Zainal Z., Yusof N. A., (2011), Photocatalytic degradation of p-Cresol by zinc oxide under UV irradiation. *Int. J. Mol. Sci.* 13: 302-315.
- [28] Nageswara Rao A., Sivasankar B., Sadasivam V., (2009), Kinetic study on the photocatalytic degradation of salicylic acid using ZnO catalyst. *J. Hazard. Mater.* 166: 1357-1361.
- [29] Monshi A., Foroughi M. R., Monshi M. R., (2012), Modified Scherrer equation to estimate more accurately nanocrystallite size using XRD. *World J. Nano Sci. Eng.* 2: 154-160.
- [30] Dos Santos T. C., Zocolo G. J., Morales D. A., De Aragão Umbuzeiro G., Zanoni M. V. B., (2014), Assessment of the breakdown products of solar/UV induced photolytic degradation of food dye tartrazine. *Food Chem. Toxicol.* 68: 307-315.
- [31] Hong R., Zhang S., Di G., Li H., Zheng Y., Ding J., Wei D., (2008), Preparation, characterization and application of Fe_3O_4/ZnO core/shell magnetic nanoparticles. *Mater. Res. Bull.* 43: 2457-2468.
- [32] Elmolla E. S., Chaudhuri M., (2010), Degradation of amoxicillin, ampicillin and cloxacillin antibiotics in aqueous solution by the UV/ZnO photocatalytic process. *J. Hazard. Mater.* 173: 445-449.
- [33] Konstantinou I. K., Albanis T. A., (2004), TiO_2 -assisted photocatalytic degradation of azo dyes in aqueous solution: Kinetic and mechanistic investigations: A review. *Appl. Catal. B.* 49: 1-14.
- [34] Assi N., Aberoomand Azar P., Saber Tehrani M., Waqif Husain S., (2016), Studies on photocatalytic performance and photodegradation kinetics of zinc oxide nanoparticles prepared by microwave assisted sol-gel technique using ethylene glycol. *J. Iran. Chem. Soc.* 13:1593-1602
- [35] Chakrabarti S., Dutta B. K., (2004), Photocatalytic degradation of model textile dyes in wastewater using ZnO as semiconductor catalyst. *J. Hazard. Mater.* 112: 269-278.
- [36] Docters T., Chovelon J. M., Herrmann J. M., Deloume J. P., (2004), Syntheses of TiO_2 photocatalysts by the molten salts method: Application to the photocatalytic degradation of Prosulfuron. *Appl. Catal. B.* 50: 219-226.
- [37] Chakrabarti S., Chaudhuri B., Bhattacharjee S., Ray A. K., Dutta B. K., (2009), Photo-reduction of hexavalent chromium in aqueous solution in the presence of zinc oxide as semiconductor catalyst. *Chem. Eng. J.* 153: 86-93.
- [38] Darwish M., Mohammadi A., Assi N., (2016), Microwave-assisted polyol synthesis and characterization of pvp-capped CdS nanoparticles for the photocatalytic degradation of tartrazine. *Mater. Res. Bull.* 74: 387-396.
- [39] Zhao H., Xu S., Zhong J., Bao X., (2004), Kinetic study on the photo-catalytic degradation of pyridine in TiO_2 suspension systems. *Catal. Today.* 93: 857-861.
- [40] Bekbölet M., Balcioglu I., (1996), Photocatalytic degradation kinetics of humic acid in aqueous TiO_2 dispersions: The influence of hydrogen peroxide and bicarbonate ion. *Water Sci. Technol.* 34: 73-80.
- [41] Gonçalves M. S. T., Pinto E. M., Nkeonye P., Oliveira-Campos A. M., (2005), Degradation of Cl reactive orange 4 and its simulated dye bath wastewater by heterogeneous photocatalysis. *Dyes Pigm.* 64: 135-139.
- [42] Sobana N., Swaminathan M., (2007), The effect of operational parameters on the photocatalytic degradation of acid red 18 by ZnO. *Sep. Purif. Technol.* 56: 101-107.
- [43] Saravanan R., Gupta V. K., Narayanan V., Stephen A., (2013), Comparative study on photocatalytic activity of ZnO prepared by different methods. *J. Mol. Liq.* 181: 133-141.
- [44] Hoffmann M. R., Martin S. T., Choi W., Bahnemann D. W., (1995), Environmental applications of semiconductor photocatalysis. *Chem. Rev.* 95: 69-96.
- [45] Dharma J., Pisal A., Shelton C., (2009), Simple method of measuring the band gap energy value of TiO_2 in the powder form using a UV/Vis/NMR spectrometer. *Appl. Note Shelton.* CT: PerkinElmer.